Hydrodynamic theory of intrasubband plasmons in quasi-one-dimensional systems

Bernardo S. Mendoza and W. L. Schaich
Department of Physics and Materials Research Institute, Indiana University, Bloomington, Indiana 47405
(Received 16 August 1990)

We use a simple hydrodynamic model to develop a theory of intrasubband plasmons in (quasi-) one-dimensional systems. The derivation gives insights into the relative motion of charge within different subbands, and the results allow easy estimates of the coupling of these modes to either internal or external charges. We compare the hydrodynamic model predictions with those of a microscopic theory, the quantum-mechanical random-phase approximation, both at a formal and at a numerical level. The phenomenological parameters can be chosen so that hydrodynamics reproduces the microscopic results in the long-wavelength limit.

I. INTRODUCTION

Advances in microfabrication techniques of semiconductors have given experimental access to systems of reduced dimensionality. For instance, the confinement of electrons to quasi-one-dimensional (Q1D) wires is now commonly achieved.[1] Among the many interesting properties that can be studied in such systems, this paper will focus on intrasubband plasmons in Q1D wires. These modes in various contexts have often been treated theoretically,[2–20] but to our knowledge there is as yet no direct experimental evidence of their existence in the new semiconductor systems. One of our aims in this and further work,[21] is to elucidate their physical nature and experimental signature.

The theoretical description of collective modes in Q1D systems has to date followed a common path based on considering the linear response to external perturbations. One derives within a mean-field approximation an effective dielectric function (or matrix) to describe the response. The singularities in the response function occur by definition at the collective modes and are located by finding the zeros in the dielectric function, or more generally in the determinant of the dielectric function matrix. This approach allows the most general evaluation of the modes' dispersion relations, but seldom gives insight into the motion of charges within or the perturbing fields produced by a single mode.

We develop in this paper a phenomenological theory of Q1D intrasubband plasmons which provides such insights via simple calculations. The equations of this theory are set up in Sec. II and their formal solution is given. Various limiting cases and features which can be described without detailed calculations are pointed out. In Sec. III we use our theory to describe the linear response. By comparing our results with the formal results of the more microscopic theories we can clarify the specific approximations that underlie our approach. Such comparisons are made quantitative in the model calculations reported in Sec. IV. Our theory is shown to provide a tractable, transparent, and reliable description of the important physics over a limited but important range of the phase space of intrasubband collective modes in Q1D wires.

This conclusion must be tempered, however, by the acknowledgement that it is being drawn by a comparison with an approximate microscopic theory, specifically the quantum-mechanical random-phase approximation. Exchange and correlation effects that are omitted by the latter are also missing from our phenomenological model. Furthermore, all the theories considered here allow for neither electron localization nor Peierls distortion along the length of the wires, and these omissions must eventually become severe in the low-frequency limit.

II. HYDRODYNAMIC MODEL

We set up our theory initially for a single wire running along the x axis. The electrons' motion is presumed to be free down the length of the wire, but to be confined in various quantum states transverse to the wire. Thus a single-particle eigenstate is written as

$$\psi_{k\alpha}(\mathbf{x})=\frac{e^{ikx}}{\sqrt{L}}\Psi_{\alpha}(X)\ , \tag{1}$$

where L is the quantization length of the wire, $X=(y,z)$ describes the coordinates transverse to the wire, and the quantum numbers are k for longitudinal motion and α for transverse motion. The separable eigenstate of (1) has an additive eigenenergy:

$$E(k,\alpha)=\frac{\hbar^2k^2}{2m}+\varepsilon_{\alpha}\ . \tag{2}$$

A basic approximation for the theories considered in this paper is to neglect the possibility of jumps between states with different values of α, i.e., to ignore intersubband transitions. This is reasonable in the limit of low excitation energies, which, as we will show in Sec. IV, is the only regime where our hydrodynamic theory is reliable.

A microscopic theory incorporating this constraint is easy to write (see Sec. III), but we first want to develop a still simpler theory based on hydrodynamic equations. Such an approach has a long history of useful applications in systems of higher dimensionality,[22–25] but we are

not aware of any previous development of it for (quasi-) one-dimensional systems. Instead of the microscopic wave functions, one bases this theory on more macroscopic quantities that are described in terms of a few "collective-coordinate" variables. The analogue of (1) is to write the density as

$$n(\mathbf{x})=\sum_{\alpha} n_{\alpha}(\mathbf{x}) , \tag{3}$$

where

$$n_{\alpha}(\mathbf{x})=n_{\alpha}(x)N_{\alpha}(X) . \tag{4}$$

Here the summation over α runs (as it shall henceforth) only over the s subbands that are partially occupied, i.e., over those α that satisfy $\varepsilon_{\alpha}<E_F$, where E_F is the Fermi energy. The $N_{\alpha}(X)=|\Psi_{\alpha}(X)|^2$ and satisfy $\int d^2X\, N_{\alpha}(X)=1$. They describe the transverse distribution of charge within a given subband. The density along x is given by $n_{\alpha}(x)=n_{\alpha}^0+\delta n_{\alpha}(x)$, which we separate into an equilibrium value, n_{α}^0, and a deviation $\delta n_{\alpha}(x)$.

The hydrodynamic model consists of a set of phenomenological equations that allow the calculation of $\delta n_{\alpha}(x,t)$ and some related functions. First, there is the equation of continuity:

$$\frac{\partial \delta\rho_{\alpha}}{\partial t}+\frac{\partial j_{\alpha}}{\partial x}=0 , \tag{5}$$

where $\delta\rho_{\alpha}=e\delta n_{\alpha}$ with $e<0$ an electron's charge, and j_{α} the 1D current density. Second, there is a (linearized) equation of motion:

$$\frac{\partial j_{\alpha}}{\partial t}=\frac{n_{\alpha}^0 e^2}{m}E_{\alpha}-\beta_{\alpha}^2\frac{\partial \delta\rho_{\alpha}}{\partial x} , \tag{6}$$

which attributes the acceleration of electrons to direct electrical forces and to density gradients. The spatial dispersion parameters β_{α} have the units of speed, and their values will be chosen later. The E_{α} in (6) is the component of the total electric field directed along the wire and averaged over the cross section of the wire: $E_{\alpha}(x)=\int d^2X\, N_{\alpha}(X)\hat{\mathbf{x}}\cdot\mathbf{E}(\mathbf{x})$. The full $\hat{\mathbf{x}}\cdot\mathbf{E}$ is found (in the electrostatic limit) from $\hat{\mathbf{x}}\cdot\mathbf{E}=-\partial\Phi/\partial x$, with the scalar potential given by

$$\Phi^{\mathrm{tot}}(\mathbf{x})=\Phi^{\mathrm{ext}}(\mathbf{x})+\int d^3x'\frac{\delta\rho(\mathbf{x}')}{|\mathbf{x}-\mathbf{x}'|} , \tag{7}$$

where we have separated the total Φ into external and induced parts and $\delta\rho=\sum_{\alpha}\delta\rho_{\alpha}$. Equations (5)–(7) and related definitions form a closed set and specify our hydrodynamic model. The key approximation lies in (6); its mathematical and physical content will be gradually revealed through the rest of the paper.

We begin by finding the eigenmode solutions of (5)–(7). To this end, set Φ^{ext} to zero and introduce the displacement (or strain) field $\xi_{\alpha}(x,t)$, which is related to $\delta n_{\alpha}(x,t)$ by

$$\delta n_{\alpha}(x,t)=-n_{\alpha}^0\frac{\partial \xi_{\alpha}}{\partial x} . \tag{8}$$

We can also express the current density in terms of ξ_{α}:

$$j_{\alpha}(x,t)=n_{\alpha}^0 e\frac{\partial \xi_{\alpha}}{\partial t} . \tag{9}$$

Together, (8) and (9) guarantee that (5) is satisfied. Next, eliminate j_{α} between (5) and (6) to find

$$\left[-\frac{\partial^2}{\partial t^2}+\beta_{\alpha}^2\frac{\partial^2}{\partial x^2}\right]\delta\rho_{\alpha}=\frac{n_{\alpha}^0 e^2}{m}\frac{\partial E_{\alpha}}{\partial x} . \tag{10}$$

Then, since we are looking for an eigenmode, we write

$$\xi_{\alpha}(x,t)=\xi_{\alpha}(q)e^{+i(qx-\omega t)} \tag{11}$$

and note that the 1D transform of the Coulomb potential is[26]

$$\int dx\, e^{-iqx}\frac{1}{|\mathbf{x}|}=2K_0(|q|\,|X|) , \tag{12}$$

where K_0 is a modified Bessel function of zeroth order.

Incorporating (8), (11), and (12) into (10) yields

$$(\omega^2-\beta_{\alpha}^2q^2)\xi_{\alpha}(q)=\sum_{\alpha'}V_{\alpha,\alpha'}(q)\omega_{\alpha'}^2\xi_{\alpha'}(q) , \tag{13}$$

where $\omega_{\alpha}^2=n_{\alpha}^0e^2q^2/m$ and

$$V_{\alpha,\alpha'}(q)=\int d^2X\int d^2X' N_{\alpha}(X)\times 2K_0(|q|\,|X-X'|)N_{\alpha'}(X') \tag{14}$$

is the dimensionless, real-valued, symmetric matrix describing the Coulomb coupling between electrons in different subbands.

If we define $\gamma_{\alpha}(q)=(n_{\alpha}^0)^{1/2}\xi_{\alpha}(q)$, we obtain an eigenvalue equation for ω^2,

$$\omega^2\gamma_{\alpha}(q)=\sum_{\alpha'}\Gamma_{\alpha,\alpha'}(q)\gamma_{\alpha'}(q) , \tag{15}$$

in which the kernel,

$$\Gamma_{\alpha,\alpha'}(q)=\beta_{\alpha}^2q^2\delta_{\alpha,\alpha'}+\sqrt{\omega_{\alpha}}V_{\alpha,\alpha'}(q)\sqrt{\omega_{\alpha'}} ,$$

is Hermitian and, hence, is diagonalized by an orthogonal matrix:

$$\Omega_{\mu}^2\delta_{\mu,\mu'}=\sum_{\alpha,\alpha'}B_{\mu\alpha}^{-1}\Gamma_{\alpha,\alpha'}B_{\alpha'\mu'} , \tag{16}$$

with $\overleftrightarrow{\mathbf{B}}^{\mathrm{tr}}=\overleftrightarrow{\mathbf{B}}^{-1}$. The collective coordinate of the μth coupled plasmon mode (for $\mu=1,\ldots,s$) is defined by

$$\eta_{\mu}(q)=\sum_{\alpha}B_{\mu\alpha}^{-1}\gamma_{\alpha}(q)=\sum_{\alpha}B_{\alpha\mu}\gamma_{\alpha}(q) , \tag{17}$$

and has eigenmode frequency $\Omega_{\mu}(q)$. Working back through the algebra, one can also say that for the μth plasmon mode the Fourier amplitude of the displacement field in the αth subband is

$$\xi_{\alpha}^{(\mu)}(q)=\frac{1}{(n_{\alpha}^0)^{1/2}}B_{\alpha\mu}\eta_{\mu}(q) . \tag{18}$$

We will solve numerically in Sec. IV a model that has $s=2$ occupied subbands. To give some analytic insight here, we simplify (13) by assuming that the N_{α} are identical so all elements in the matrix $V_{\alpha,\alpha'}(q)$ have the same value, $V_c(q)>0$. Then (13) becomes an eigenvalue equation with a separable kernel and the eigenvalue ω^2 obeys

$$1/V_c(q)=\sum_\alpha \frac{\omega_\alpha^2}{\omega^2-\beta_\alpha^2 q^2}\equiv F(\omega^2)\ , \tag{19}$$

whose solutions are easily visualized by graphical means. In Fig. 1 we schematically illustrate a case with $s=5$ occupied subbands.[27] The one solution whose ω is greater than all the $\beta_\alpha q$ we call the Q1D plasmon. It is always present and everyone's theory has it. The other solutions are "trapped" between successive values of $\beta_\alpha q$ and are only present if $s\geq 2$. These additional modes were first discovered theoretically by Lee, Ulloa, and Lee,[6] who called them slender acoustic plasmons. They have received less attention[6,15–17,20] because they require multiple-subband occupancy, but they are a novel feature of Q1D systems since there alone do they avoid Landau damping. The analogue of (18) for a system with $V_{\alpha,\alpha'}\to V_c$ is

$$\xi_\alpha^{(\mu)}(q)\propto[\Omega_\mu^2(q)-\beta_\alpha^2 q^2]^{-1}\ , \tag{20}$$

which has all the qualitative features described by Lee, Ulloa, and Lee. Specifically, for the Q1D plasmon mode all the ξ_α's have the same sign, while for the remaining $s-1$ modes the sign of ξ_α depends (only) on whether $\Omega_\mu(q)$ is bigger or smaller than $\beta_\alpha q$. The in-phase motion of the subband plasmons in the Q1D plasmon mode implies that it will more strongly interact with perturbing charges or fields than will the other modes whose subband motions are partially out of phase.

To make this last claim quantitative we return to the formal development of the hydrodynamic model. We want to move from a classical mechanical equation of motion, such as (13), to a quantum-mechanical Hamiltonian description.[23,28] Begin by considering the classical Hamiltonian

$$\begin{aligned}H&=\int d^3x\tfrac{1}{2}m\sum_\alpha N_\alpha(X)n_\alpha^0\left[\left[\frac{\partial\xi_\alpha}{\partial t}\right]^2+\beta_\alpha^2\left[\frac{\partial\xi_\alpha}{\partial x}\right]^2\right]\\&\quad+\frac{e^2}{2}\int d^3x\int d^3x'\sum_{\alpha,\alpha'}\frac{\delta n_\alpha(\mathbf{x})\delta n_{\alpha'}(\mathbf{x}')}{|\mathbf{x}-\mathbf{x}'|}\\&=\int dx\tfrac{1}{2}m\sum_\alpha n_\alpha^0\left[\left[\frac{\partial\xi_\alpha}{\partial t}\right]^2+\beta_\alpha^2\left[\frac{\partial\xi_\alpha}{\partial x}\right]^2\right]\\&\quad+\frac{e^2}{2}\int dx\int dx'\sum_{\alpha,\alpha'}\delta n_\alpha(x)V_{\alpha,\alpha'}(x,x')\delta n_{\alpha'}(x')\ ,\end{aligned} \tag{21}$$

where

$$V_{\alpha,\alpha'}(x,x')=\int d^2X\int d^2X' N_\alpha(X)\frac{1}{|\mathbf{x}-\mathbf{x}'|}N_{\alpha'}(X')\ . \tag{22}$$

Applying Hamilton's equations of motion [using (8)] yields

$$\begin{aligned}mn_\alpha^0\frac{\partial^2\xi_\alpha}{\partial t^2}&=m\beta_\alpha^2 n_\alpha^0\frac{\partial^2\xi_\alpha}{\partial x^2}\\&\quad+e^2n_\alpha^0\sum_{\alpha'}\int dx'\frac{\partial}{\partial x}V_{\alpha,\alpha'}(x,x')\frac{\partial\xi_{\alpha'}}{\partial x'}(x')n_\alpha^0\ .\end{aligned} \tag{23}$$

If we assume a solution of the form (11), (23) reduces quickly to (13), so the H of (21) is an equivalent representation of the hydrodynamic model.

We next quantize this Hamiltonian. If we replace $\xi_\alpha(x,t)$ with

$$[1/(n_\alpha^0)^{1/2}]\sum_\mu B_{\alpha\mu}\eta_\mu(q,t)\ ,$$

we obtain (with overdots denoting time derivatives)

$$H=\frac{mL}{2}\sum_q\sum_\mu[\dot\eta_\mu(q)\dot\eta_\mu(-q)+\Omega_\mu^2(q)\eta_\mu(q)\eta_\mu(-q)]\ , \tag{24}$$

which is of harmonic oscillator form and can be quantized by writing

$$\eta_\mu(q)=\left[\frac{\hbar}{2mL\Omega_\mu(q)}\right]^{1/2}[a_\mu(q)+a_\mu^\dagger(-q)] \tag{25}$$

and imposing the commutation relations

$$[a_\mu(q),a_{\mu'}^\dagger(q')]=\delta_{\mu,\mu'}\delta_{q,q'},\quad [a_\mu(q),a_{\mu'}(q')]=0\ . \tag{26}$$

Then (24) becomes

$$\hat H=\sum_q\sum_\mu\hbar\Omega_\mu(q)[a_\mu^\dagger(q)a_\mu(q)+\tfrac{1}{2}]\ , \tag{27}$$

where the caret is a reminder that $\hat H$ is now an operator. Working back through the algebra, we can also write the electron density as an operator:

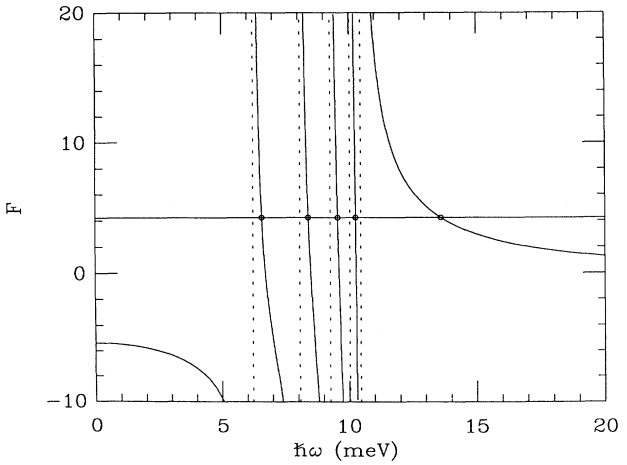

FIG. 1. Superimposed plots of the left- and right-hand sides of Eq. (19) vs frequency at $q=10^5$ cm^{-1}. System parameters are from Ref. 27 and incorporate an m^* and a background ε_0. The vertical dashed lines are the asymptotes of the divergences; their locations are set by $\omega=\beta_\alpha q$ for $\alpha=1,2,3,4,5$. The horizontal line is $\varepsilon_0/V_c(q)$ and the circles are the solutions of Eq. (19).

$$\delta\hat{n}(\mathbf{x},t)=\sum_q(-iq)e^{iqx}\sum_\alpha N_\alpha(X)(n_\alpha^0)^{1/2}\times\sum_\mu B_{\alpha\mu}\left[\frac{\hbar}{2mL\Omega_\mu(q)}\right]^{1/2}\times[a_\mu(q,t)+a_\mu^\dagger(-q,t)]\ , \quad (28)$$

which can be used to determine how the plasmons scatter single electrons either inside[29] or outside the wire.

We will demonstrate the utility of (28) in the next section, but to end this section we briefly describe how our analysis may be generalized if more than one wire is present. We assume the wires are identical and parallel and that there is no tunneling of electrons between them. Then the only change in (13) is the appearance of indices to indicate which wire is meant:

$$(\omega^2-\beta_\alpha^2q^2)\xi_{\alpha,l}(q)=\sum_{\alpha',l'}V_{\alpha,\alpha';l,l'}(q)\omega_{\alpha'}^2\xi_{\alpha',l'}(q)\ , \quad (29)$$

where

$$V_{\alpha,\alpha';l,l'}(q)=\int d^2X\int d^2X'N_\alpha(X-X_l)\times2K_0(|q|\,|X-X'|)\times N_{\alpha'}(X'-X_{l'})\ , \quad (30)$$

and X_l is the location of the lth wire in the (y,z) plane. If the array of wires is periodic, we can assume

$$\xi_{\alpha,l}(q)=\xi_\alpha(\mathbf{q})e^{iQ\cdot X_l}\ , \quad (31)$$

which converts (29) to

$$(\omega^2-\beta_\alpha^2q^2)\xi_\alpha(\mathbf{q})=\sum_\alpha V_{\alpha,\alpha'}(\mathbf{q})\omega_{\alpha'}^2\xi_{\alpha'}(\mathbf{q})\ , \quad (32)$$

where

$$V_{\alpha,\alpha'}(\mathbf{q})=\sum_{l'}e^{-iQ\cdot(X_l-X_{l'})}V_{\alpha,\alpha';l,l'}(q)=V_{\alpha',\alpha}(\mathbf{q})\ . \quad (33)$$

Note that Eq. (32) has the same form as (13). If the wires are well separated and $|\mathbf{q}|$ is not small, $V_{\alpha,\alpha'}(\mathbf{q})$ will be dominated by the $l'=l$ contribution in (33), which is the $V_{\alpha,\alpha'}(q)$ of (14). The formal solution of (32), the inference and quantization of an effective Hamiltonian, and the expression of the density operator in terms of plasmon modes can be done in the same fashion as for the single-wire case.[21] Our only detailed comment concerns the $|\mathbf{q}|\to0$ limit, where the elements of $V_{\alpha,\alpha'}(\mathbf{q})$ all tend to a common, divergent function $V_c(\mathbf{q})$. In view of (19) this limit leads to the largest eigenvalue being at $\omega^2\approx V_c(\mathbf{q})\sum_\alpha\omega_\alpha^2$ as $|\mathbf{q}|\to0$. It is interesting to note the specific limiting form as $|\mathbf{q}|\to0$ of

$$V_c(\mathbf{q})\to\begin{cases}2\pi/d\,|\mathbf{q}| & \text{in two dimensions,}\\ 4\pi/A\,|\mathbf{q}|^2 & \text{in three dimensions,}\end{cases} \quad (34)$$

where d is the wire spacing in two dimensions and A is the unit-cell area of the wire array in three dimensions. Using (34) yields, for zero transverse wave vector and $q\to0$,

$$\omega^2\to\begin{cases}\dfrac{2\pi e^2(n^0/d)|q|}{m} & \text{in two dimensions,}\\ \dfrac{4\pi e^2(n^0/A)}{m} & \text{in three dimensions,}\end{cases} \quad (35)$$

which are the standard bulk plasmons in two and three dimensions. The opposite order of limits, $q=0$ and $Q\to0$, gives zero, which shows the strong anisotropy of the wire array even in the long-wavelength limit.

III. LINEAR RESPONSE

We now consider how a single-wire system responds to a weak external perturbation. Formally the Fourier component of the induced density may be written as

$$\langle\delta n(\mathbf{x},\omega)\rangle=\int d^3x'\chi(\mathbf{x},\mathbf{x}';\omega)V^{\text{ext}}(\mathbf{x}',\omega)\ , \quad (36)$$

and there are several theoretical paths to the susceptibility χ. Perhaps the easiest, given (28), is to use the Kubo formula,[30]

$$\chi(\mathbf{x},\mathbf{x}';\omega)=\frac{1}{i\hbar}\int_0^\infty d\tau\,e^{i\omega\tau}\langle\langle[\delta\hat{n}(\mathbf{x},t),\delta\hat{n}(\mathbf{x}',0)]\rangle\rangle\ , \quad (37)$$

where the square brackets denote a commutator and the double angular brackets denote a thermal average. A simple reduction leads to

$$\chi(\mathbf{x},\mathbf{x}';\omega)=\frac{1}{L}\sum_q e^{iq(x-x')}\sum_{\alpha,\alpha'}N_\alpha(X)\chi_{\alpha,\alpha'}(q,\omega)N_{\alpha'}(X') \quad (38)$$

with

$$\chi_{\alpha,\alpha'}(q,\omega)=\sum_\mu B_{\alpha\mu}B_{\alpha'\mu}\frac{q^2(n_\alpha^0n_{\alpha'}^0)^{1/2}/m}{\omega^2-\Omega_\mu^2(q)}\ . \quad (39)$$

Clearly the response is singular when the driving frequency ω matches an eigenvalue of the plasmons. Indeed, within the hydrodynamic model developed here, those are the only frequencies where energy absorption is possible.

To contrast this result with the predictions of a microscopic theory, we review the random-phase approximation (RPA) for χ. This is derived in a two-step process. One first calculates the susceptibility, χ^0, produced by independent particles. For wave functions of the form (1) and with no intersubband transitions allowed, we find that $\chi^0(\mathbf{x},\mathbf{x}';\omega)$ can be expressed as in (38), where $\chi^0_{\alpha,\alpha'}(q,\omega)=\chi^0_\alpha(q,\omega)\delta_{\alpha,\alpha'}$ with

$$\chi^0_\alpha(q,\omega)=\frac{2}{L}\sum_{\substack{k\\(k'=k+q)}}f_{k\alpha}\frac{2(\varepsilon_k-\varepsilon_{k'})}{2(\varepsilon_k-\varepsilon_{k'})^2-(\hbar\omega)^2}\ , \quad (40)$$

where $\varepsilon_k=\hbar^2k^2/2m$ and $f_{k\alpha}$ is the Fermi occupation function. The outside factor of 2 is due to the sum over spin. Evaluation of χ^0_α at zero or finite[16] temperature is straightforward.

In the second step one invokes a mean-field argument to write (schematically)

$$\begin{aligned}\langle \delta n \rangle \equiv \chi V^{\text{ext}} &= \chi^0 V^{\text{tot}} = \chi^0 (V^{\text{ext}} + V^{\text{ind}}) \\ &= \chi^0 (V^{\text{ext}} + V\langle \delta n \rangle) \\ &= \chi^0 (1 + V\chi) V^{\text{ext}} \ . \end{aligned} \tag{41}$$

Thus χ is to be found from the solution of the integral equation

$$\chi = \chi^0 + \chi^0 V \chi \ . \tag{42}$$

In a RPA theory the coupling function V is simply the Coulomb potential energy between two charges. The separable form of χ^0 leads to an easy solution of (42). We find that χ^{RPA} can also be written as in (38) with

$$\chi^{\text{RPA}}_{\alpha,\alpha'}(q,\omega) = \chi^0_\alpha (\overleftrightarrow{1} - e^2 \overleftrightarrow{V} \cdot \overleftrightarrow{\chi}^0)^{-1}_{\alpha,\alpha'} \ , \tag{43}$$

where the matrices are indexed by the (occupied) α's and $V_{\alpha,\alpha'}(q)$ is given by (14).

A hydrodynamic calculation of χ can be done along the same lines. The second step will be formally identical, so we only need the hydrodynamic χ^0. This function is readily found from the basic hydrodynamic equations. (5)–(7); we simply do not separate Φ^{tot}. The answer again has the form (38), but now with $\chi^{0,H}_{\alpha,\alpha'}(q,\omega) = \chi^{0,H}_\alpha(q,\omega)\delta_{\alpha,\alpha'}$, where

$$\chi^{0,H}_\alpha(q,\omega) = \frac{\omega_\alpha^2/e^2}{\omega^2 - \beta_\alpha^2 q^2} \ . \tag{44}$$

Thus, to the extent that (44) mimics (40), our hydrodynamic theory will be reliable. To aid this comparison we choose the β_α's so that at zero temperature the two χ^0's agree as $\omega \to 0$ and as $\omega \to \infty$. This is accomplished by setting β_α equal to the Fermi velocity of electrons in the αth subband:

$$\beta_\alpha = \left[\frac{2}{m}(E_F - \varepsilon_\alpha) \right]^{1/2} \ . \tag{45}$$

Only in one dimension can a single choice of β_α reproduce *both* the high- and low-frequency limits of χ^0_α.

However, the choice of the β_α does not restore the continuum of single-particle excitations missing in (44). To show the consequences of this omission we examine a simple electron-energy-loss spectrum (EELS) in which an external electron is bounced off a single wire. This is to be thought of as a *gedanken* experiment; allowance for the many additional complications of a real experiment is given elsewhere.[21] We will calculate the EELS assuming long-range dipole coupling and a fixed trajectory for the probe electron. As with χ, there are several possible theoretical approaches and all of them need an expression for the external potential produced by the probe. Using (12) this may be written as

$$\begin{aligned}\Phi^{\text{ext}}(\mathbf{x},t) = \frac{e}{L}\sum_q e^{iq[x - x(t)]} \\ \times 2K_0(|q|\{[y - y(t)]^2 + [z - z(t)]^2\}^{1/2}) \ . \end{aligned} \tag{46}$$

We assume the probe electron moves in the $y = 0$ plane (where the wire also lies) and reflects "specularly" from the wire at $t = 0$. The probe's velocity is described by $\mathbf{v}(t) = (v_x, 0, v_z \text{sgn} t)$. To match the model in Sec. IV, the wire is presumed to have negligible thickness along $\hat{\mathbf{z}}$, so the transverse states are only nontrivial functions of y. Incorporating these assumptions into (46) and forming its time Fourier transform, we find, at $z = 0$ and averaged over a transverse state, that

$$\Phi^{\text{ext}}_\alpha(x,\omega) = \frac{e}{L}\sum_q e^{iqx} f_\alpha(q,\omega,\mathbf{v}) \ , \tag{47}$$

with

$$\begin{aligned} f_\alpha(q,\omega,\mathbf{v}) = \int dy \, N_\alpha(y) \int dt \, e^{i(\omega - q v_x)t} \\ \times 2K_0[|q|(y^2 + v_z^2 t^2)^{1/2}] \end{aligned} \tag{48}$$

is the quantity that perturbs electrons in the αth subband.

The simplest way to find its effect in the hydrodynamic model is to combine (46) and (28) into a time-dependent perturbation

$$\hat{H}'(t) = e^2 \int d^3x \, \delta\hat{n}(\mathbf{x},0)\Phi^{\text{ext}}(\mathbf{x},t) \ , \tag{49}$$

which at frequency ω appears as

$$\begin{aligned}\hat{H}'(\omega) &= e^2 \sum_q \sum_\alpha iq f_\alpha(q,\omega,\mathbf{v}) \sum_\mu B_{\alpha\mu} \left[\frac{\hbar n^0_\alpha}{2mL\Omega_\mu(q)} \right]^{1/2} \\ &\quad \times [a_\mu(-q) + a^\dagger_\mu(q)] \\ &= \sum_q \sum_\mu M_{q,\mu}(\omega)[a_\mu(-q) + a^\dagger_\mu(q)] \ . \end{aligned} \tag{50}$$

Combining (27) and (50), we have the so-called driven boson model, whose solution is well known.[31] The probability at zero temperature of a single loss event over the course of the trajectory can be expressed as

$$P_1 = \int_0^\infty d\omega \int_{-\infty}^\infty dq \, P_1(q,\omega) \ , \tag{51}$$

where

$$P_1(q,\omega) = \frac{L}{2\pi\hbar^2}\sum_\mu |M_{q,\mu}(\omega)|^2 \delta(\omega - \Omega_\mu(q)) \ . \tag{52}$$

Allowance for finite temperature and for multiple losses and gains is also easily done in this model,[31,32] but we stop at this level in order to compare with a linear-response estimate.

The latter is found from the dielectric theory of EELS.[33] This proceeds by first finding the induced charge density due to Φ^{ext}. With the same assumptions as for the driven boson model, we obtain, from (36) and (38),

$$\langle \delta\rho(\mathbf{x},\omega) \rangle = \frac{1}{L}\sum_q \sum_\alpha e^{iqx} N_\alpha(y)\delta(z)\rho_\alpha(q,\omega,\mathbf{v}) \ , \tag{53}$$

where

$$\rho_\alpha(q,\omega,\mathbf{v}) = e^3 \sum_{\alpha'} \chi_{\alpha,\alpha'}(q,\omega) f_{\alpha'}(q,\omega,\mathbf{v}) \ . \tag{54}$$

One next calculates the work done against the probe

charge by the field produced by the induced charge density:

$$W=-\int_{-\infty}^{\infty} dt\ \mathbf{v}(t)\cdot\mathbf{F}^{\text{ind}}(t)\ , \tag{55}$$

where

$$\mathbf{F}^{\text{ind}}(t)=-e\nabla\Phi^{\text{ind}}(\mathbf{x})|_{\mathbf{x}=\mathbf{x}(t)}\ . \tag{56}$$

The connection to the loss probability in (51) comes from writing

$$W=\int_0^{\infty} d\omega\,\hbar\omega\int_{-\infty}^{\infty} dq\ P_1(q,\omega)\ . \tag{57}$$

After some straightforward algebra we can identify, as the linear-response estimate of P_1,

$$P_1(q,\omega)=\frac{e^2}{2\pi\hbar}\sum_{\alpha,\alpha'} f_\alpha(q,\omega,\mathbf{v}) \times\left[-\text{Im}\left[\frac{e^2}{\pi}\chi_{\alpha,\alpha'}(q,\omega)\right]\right] \times f_{\alpha'}(q,\omega,\mathbf{v})\ , \tag{58}$$

where Im denotes "imaginary part of." A numerical comparison of (52) and (58) will be developed in the next section.

IV. MODEL CALCULATION

In order to illustrate quantitatively the strengths and weaknesses of our hydrodynamic model, we set up a detailed calculation using typical parameter values. The potential well confining the electrons to the wire is presumed to have a rectangular cross section of extent $a=400$ Å in the y direction and much narrower in the z direction. The barrier shape is that of an infinite square well, so

$$N_\alpha(X)\approx\frac{2}{a}\delta(z)\sin^2\left[\frac{\alpha\pi}{a}\left[y+\frac{a}{2}\right]\right]\ , \tag{59}$$

where $\alpha=1$, 2, etc. With InSb in mind,[34] we replace the free-electron mass m with $m^*=0.014m$ and screen factors of e^2 to e^2/ε_0, where $\varepsilon_0=17.7$. The transverse bound-state energies, measured from the bottom of the well, are then

$$\varepsilon_\alpha=\frac{\hbar^2(\alpha\pi/a)^2}{2m^*}\ , \tag{60}$$

and we choose the Fermi energy so two subbands are partially occupied and contain a total 1D density of $n^0=1.6\times10^6\ \text{cm}^{-1}=n_1^0+n_2^0$. This requires $E_F=89$ meV, while the subband parameters are $\varepsilon_\alpha=16.8$ (67.3) meV, $n_\alpha^0=1.03$ $(0.57)\times10^6$ cm^{-1}, and $\beta_\alpha=13.5$ $(7.9)\times10^7$ cm/s for $\alpha=1$ (2).

Figure 2 compares the hydrodynamic and microscopic predictions of the two plasmon modes that can exist in this system. In the small-q limit the agreement is excellent, by design. At larger q, specifically as the microscopic dispersion curves bend upward to avoid the single-particle continuum, the hydrodynamic predictions move directly into these regions of Landau damping and become meaningless. We did not plot the microscopic RPA modes over their full q range of existence because they move indistinguishably close to the continuum boundaries. The upper mode never actually touches the boundary,[2] but the lower one does make contact and stops at the end of the gap in the single-particle continuum, which occurs here at $q=7.4\times10^5$ cm^{-1} and $\hbar\omega=50.6$ meV. Of course, the hydrodynamic model misses these subtle behaviors at large q.

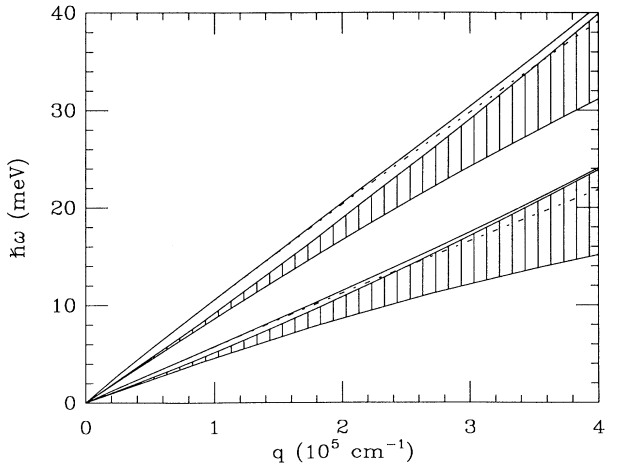

FIG. 2. Dispersion of the intrasubband plasmons for a system with two partially occupied subbands. The microscopic RPA results are the solid lines, while the hydrodynamic predictions are the dashed lines. Also shown as the vertically striped area is the region of allowed single-particle excitations; the gap through the middle of it is crucial for the existence of the lower plasmon mode. See text for specific parameter choices.

To compare the different solutions further, we also consider their estimates of the *gedanken* EELS derived in

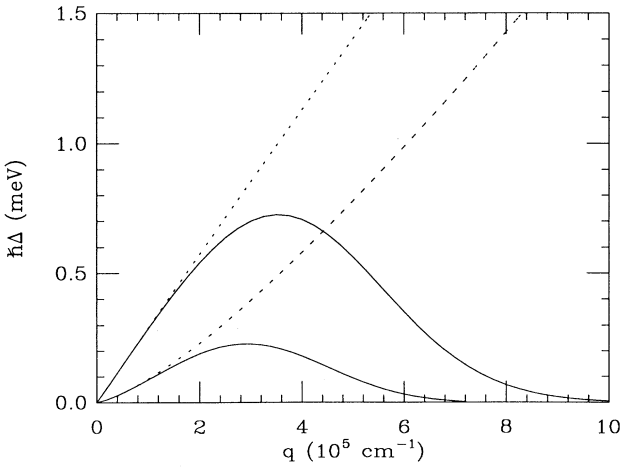

FIG. 3. Coupling function Δ vs wave vector q. The solid lines are microscopic RPA results and the dashed lines are hydrodynamic predictions. The stronger Δ's correspond to the upper modes in Fig. 1 and the weaker Δ's to the lower.

Sec. III, or, more precisely, the strength of the δ-function peaks in the EEL spectrum. This comparison can be simplified if one neglects the (weak) α dependence of the $f_\alpha(q,\omega,\mathbf{v})$ in (48). Then the quantities to contrast are

$$P_1^{(H)}(q,\omega)=\frac{e^2/\varepsilon_0}{2\pi\hbar}f^2(q,\omega,\mathbf{v}) \times\sum_\mu \Delta^{(H)}(q,\mu)\delta(\omega-\Omega_\mu(q)) , \quad (61)$$

with

$$\Delta^{(H)}(q,\mu)=\frac{e^2q^2/\varepsilon_0}{2m^*\Omega_\mu(q)}\left|\sum_\alpha (n_\alpha^0)^{1/2}B_{\alpha\mu}\right|^2 , \quad (62)$$

versus

$$P_1^{(\mathrm{RPA})}(q,\omega)=\frac{e^2/\varepsilon_0}{2\pi\hbar}f^2(q,\omega,\mathbf{v}) \times\sum_\mu \Delta^{(\mathrm{RPA})}(q,\mu)\delta(\omega-\Omega_\mu(q)) , \quad (63)$$

with

$$\Delta^{(\mathrm{RPA})}(q,\mu)=\left|\frac{\partial g}{\partial\omega}\right|^{-1}_{\omega=\Omega_\mu(q)} , \quad (64)$$

where

$$\sum_{\alpha,\alpha'}\mathrm{Im}\left[\frac{e^2}{\varepsilon_0}\chi^{(\mathrm{RPA})}_{\alpha,\alpha'}(q,\omega)\right]=1/g(q,\omega) . \quad (65)$$

The $\Delta^{(\mathrm{RPA})}$'s describe the residues of the poles in $1/g$; we are ignoring the smooth contribution of single-particle excitations to (58). To avoid choosing a particular $\mathbf{v}$, we compare in Fig. 3 the hydrodynamic and microscopic RPA predictions of Δ. Again, the agreement is excellent in the low-q range, but serious discrepancies develop for the same q where the mode dispersions differ. The range of q plotted is greater than in Fig. 2 to show how at high frequencies the microscpic coupling to plasmons becomes negligible because most of the absorption strength is going into the single-particle continuum. Indeed, the difference at a fixed q between the hydrodynamic Δ and the microscopic one is a measure of the importance of such excitations. As for the EELS, the comparison between the two theories is better than Fig. 3 would suggest because $|f^2|$ varies roughly as q^{-2}, so the P_1's are largest in the low-q region, where there is a common prediction of Δ.

A final point to note about Fig. 3 is the larger size of Δ for the upper mode than for the lower. This feature is easy to understand in the hydrodynamic model as being due to the relative phase of the charge motion in the different subbands. From the general discussion in Sec. II, we expect and find that $B_{1\mu}/B_{2\mu}$ is positive for the upper mode and negative for the lower, thus rationalizing the different magnitudes of $\Delta^{(H)}$ calculated from (62). A similar qualitative argument has been made before in a microscopic theory,[16] but it could not be used for quantitative estimates. Such a possibility is one of the special advantages of the hydrodynamic model.

ACKNOWLEDGMENTS

This work was supported in part by the National Science Foundation under Grant No. DMR-89-03851. One of us (B.M.S.) would like to thank Y. C. Lee and G. Canright for helpful discussions.

[1]Rather than specific articles, we list several conference proceedings where many examples and further references can be found: *Interfaces, Quantum Wells, and Superlattices,* edited by C. R. Leavens and R. Taylor (Plenum, New York, 1988); *Nanostructure Physics and Fabrication,* edited by M. A. Reed and W. P. Kirk (Academic, New York, 1989); Surf. Sci. **228** (1990); **229** (1990).
[2]P. F. Williams and A. N. Bloch, Phys. Rev. B **10**, 1097 (1974).
[3]M. Apostol, Z. Phys. B **22**, 279 (1975).
[4]V. B. Campos, O. Hipólito, and R. Lobo, Phys. Status Solidi B **81**, 657 (1977).
[5]W. I. Friesen and B. Bergersen, J. Phys. C **13**, 6627 (1980).
[6]Y. C. Lee, S. E. Ulloa, and P. S. Lee, J. Phys. C **16**, L995 (1983).
[7]J. Lee and H. Spector, J. Appl. Phys. **57**, 366 (1984).
[8]M Tsukada, H. Ishida, and N. Shima, Phys. Rev. Lett. **53**, 376 (1984).
[9]S. Das Sarma and W.-Y. Lai, Phys. Rev. B **32**, 1401 (1985).
[10]H. Ishida, N. Shima, and M. Tsukada, Phys. Rev. B **32**, 6246 (1985).
[11]A. K. Das, J. Phys. F **16**, L99 (1986).
[12]W.-Y. Lai, A. Kobayashi, and S. Das Sarma, Phys. Rev. B **34**, 7380 (1986).
[13]H. Chen, Y. Zhu, and S. Zhou, Phys. Rev. B **36**, 8189 (1987).
[14]Y. Zhu, F.-Y. Huang, X.-M. Xiong, and S.-X. Zhou, Phys. Rev. B **37**, 8992 (1988).
[15]Q. Li and S. Das Sarma, Phys. Rev. B **40**, 5860 (1989).
[16]B. S. Mendoza and Y. C. Lee, Phys. Rev. B **40**, 12 063 (1989).
[17]Q. Li and S. Das Sarma, Phys. Rev. B **41**, 10 268 (1990).
[18]F. Y. Huang, Phys. Rev. B **41**, 12 957 (1990).
[19]G. Y. Hu and R. F. O'Connell, Phys. Rev. B **42**, 1290 (1990).
[20]H. Yu and J. C. Hermanson, Phys. Rev. B **42**, 1496 (1990).
[21]B. S. Mendoza and W. L. Schaich (unpublished).
[22]A. L. Fetter, Ann. Phys. (N.Y.) **81**, 373 (1973); **88**, 1 (1974).
[23]G. Barton, Rep. Prog. Phys. **42**, 963 (1979).
[24]A. D. Boardman, in *Electromagnetic Surface Modes,* edited by A. D. Boardman (Wiley, New York, 1982), p. 1.
[25]F. Forstmann and R. Gerhardts, *Metal Optics Near the Plasma Frequency* (Springer, Berlin, 1986).
[26]I. S. Gradshteyn and I. M. Ryzhik, *Table of Integrals, Series and Products* (Academic, New York, 1980), Eq 3.754.2.
[27]S. E. Ulloa, Y. C. Lee, and B. S. Mendoza, in *Nanostructure Physics and Fabrication,* edited by M. A. Reed and W. P. Kirk (Academic, New York, 1989), p. 141.
[28]W. L. Schaich, Phys. Rev. B **31**, 3409 (1985).
[29]Y. C. Lee and B. S. Mendoza, Phys. Rev. B **39**, 4776 (1989); Y.

C. Lee, B. S. Mendoza, and S. E. Ulloa, Supercond. Sci. Technol. **1**, 352 (1989); B. S. Mendoza and Y. C. Lee, Phys. Rev. B **40**, 10 946 (1989).
[30]R. Kubo, J. Phys. Soc. Jpn. **12**, 570 (1957).
[31]A. A. Lucas and M. Sunjic, Prog. Surf. Sci. **2**, 75 (1972).
[32]W. L. Schaich, Surf. Sci. **122**, 175 (1982).
[33]W. L. Schaich, Phys. Rev. B **24**, 686 (1981).
[34]W. Hansen *et al.*, Phys. Rev. Lett. **58**, 2586 (1987).